Radar-Based Vibration Frequency Recovery Using mmWave

Clara Cong
Carnegie Mellon University
zcong@andrew.cmu.edu

Abstract

Vibration sensing is crucial for a wide range of applications, from structural monitoring to industrial inspection. In this work, we explore the use of mmWave radar to detect and recover the frequency of vibrations without relying on traditional Fourier-based methods, which often struggle with non-linear or high-frequency motions. Instead, we directly analyze the raw in-phase and quadrature (I/Q) signals captured before Doppler processing. To validate our approach, we adopt a controlled experiment using a Chladni plate driven by a motor with adjustable frequency and amplitude. A synchronized multi-sensor rig comprising a radar, camera, and LiDAR enables comprehensive data collection, although radar serves as the primary sensing modality. Through a series of experiments, we demonstrate that periodic vibrations manifest as characteristic signatures in the radar's raw signal and Range-Doppler domain. Furthermore, we show that the vibration frequency can be accurately recovered by analyzing the temporal patterns in the raw radar data. Our findings highlight the potential of mmWave radar as a low-cost, non-contact solution for high-precision vibration analysis.

1. Introduction

Understanding the vibration frequency of physical objects is crucial in numerous real-world scenarios, such as predictive maintenance, structural monitoring, and security sensing. Traditional vibration sensing typically relies on contact-based sensors like accelerometers or expensive laser vibrometers [9], both of which are limited in scalability, cost, and deployment flexibility. Recent advances have explored wireless alternatives using acoustic signal[5, 6] or radio frequency (RF) signal, but these methods often struggle with low sensitivity or resolution—especially when detecting fine-grained vibrations at the micrometer level.

This project proposes to explore a method for recovering the vibration frequency of objects using mmWave radar. Specifically, we investigate whether the radar signal's phase information can be leveraged to accurately infer frequency characteristics of vibrating targets. This approach is inspired by mmVib [4], a recent system that demonstrated the ability to extract sub-millimeter vibration signals using commodity mmWave devices. However, unlike mmVib's broader scope that attempts to reconstruct full vibration signals, this project focuses on a more tractable subgoal: estimating vibration frequency. By narrowing the problem, we aim to systematically validate whether frequency estimation alone is robust under real-world noise, occlusion, and sensor interference. If successful, this capability would provide practical value for applications such as industrial equipment monitoring, where abnormal vibration frequencies often precede mechanical failures. In contrast to visual methods, radar systems can operate in low light and penetrate certain occlusions and remain stable in a variety of environments. The main contribution of this project is to adapt and simplify mmVib's signal modeling framework for reliable frequency estimation. In the long run, this vibration frequency estimation can be integrated with a 3D scene reconstruction pipeline for applications such as detecting which vehicles are starting based on micro-vibrations in a parking lot or locating active machines in a cluttered environment.

2. Related Works

Vibration frequency sensing using wireless and radar technologies has attracted growing interest due to its potential for contactless and scalable deployment. Traditional vibration sensing relies on contact-based devices like accelerometers or laser vibrometers[9], which offer high accuracy but are expensive, and difficult to install in large-scale environments. In response, researchers have explored RF-based alternatives. WiFi-based systems such as WiSee [8] and WiVibe [1] enable coarse-grained motion and vibration sensing through Doppler shifts or CSI (channel state information) variations, but are fundamentally limited by WiFi's centimeter-level wavelength, which reduces their sensitivity to fine-grained displacements. Acoustic-based systems like EchoTrack [2] and VibSense[7] provide better resolution but are susceptible to ambient noise and require strict environmental conditions.

Recent advances in mmWave radar have significantly improved vibration sensing due to its millimeter-level wavelength, enabling micrometer-scale displacement detection. Works such as MilliSonic [10] and mmSense [3] use phase tracking and FMCW radar for high-resolution motion or displacement tracking, yet many of these systems focus on tracking moving targets rather than analyzing subtle, periodic vibrations. MmEye [11] extends these methods to object classification but doesn't explicitly extract vibration frequency. The most relevant work, mmVib [4], introduces a robust pipeline for recovering micrometer-scale vibrations using commercial mmWave devices. It uses a multi-signal consolidation (MSC) model to enhance robustness to multipath and noise, and demonstrates precise vibration signal recovery even in low SNR settings.

Our proposed work builds directly on mmVib, but narrows its scope to focus on the estimation of vibration frequency rather than full signal reconstruction. This distinction allows us to analyze the feasibility and reliability of extracting frequencies under different conditions. While mmVib explored frequency as part of its evaluation, it did not center frequency estimation as the core objective. Our project aims to fill this gap by simplifying the sensing pipeline and systematically analyzing how well vibration frequency can be recovered using mmWave radar under real-world challenges like multipath interference, clutter, and background motion.

3. Methods

In this section, we present the methods developed for vibration frequency recovery using mmWave radar. We begin by introducing the necessary background on FMCW radar sensing and standard velocity estimation pipelines, which lays the foundation for understanding conventional radar processing. Building on this, we explain the limitations of Doppler FFT analysis when dealing with high-frequency vibrational motion, motivating the need for a time-domain approach based on raw IQ signals. Finally, we describe how we leverage the temporal structures in the IQ data to detect and recover object vibrations without relying on Fourier-based methods.

3.1. Preliminaries

FMCW Radar Fundamentals. Frequency-Modulated Continuous Wave (FMCW) radar is a class of radar system that transmits a continuous waveform whose frequency increases linearly over time—a signal known as a chirp [5]. The transmitted chirp reflects off targets in the environment and is received by the radar system with a time delay proportional to the target's distance. Mixing the transmitted and received signals yields an intermediate frequency (IF) signal whose frequency encodes the round-trip delay and thus the target's range. If the object is stationary, the IF signal appears as a single sinusoid with constant frequency determined by the distance d, slope S, and speed of light c:

$$f_{IF} = \frac{2dS}{c} \tag{1}$$

This principle allows FMCW radars to resolve both range and velocity using purely analog processing followed by digital signal processing.

Velocity Measurement in FMCW Radar. Velocity is typically estimated by transmitting multiple chirps in sequence and analyzing the phase change across chirps. Consider two chirps separated by time T_c. The reflected signals from a moving object will undergo a phase shift between consecutive chirps due to Doppler motion. This phase shift $\Delta\phi$ is directly related to the target's radial velocity v as follows:

$$\Delta\phi = \frac{4\pi v T_c}{\lambda} \tag{2}$$

As a result, we can get:

$$v = \frac{\lambda\Delta\phi}{4\pi T_c} \tag{3}$$

where λ is the radar wavelength. This method assumes linear motion during the inter-chirp period and provides robust velocity estimates when the motion is approximately constant.

To resolve multiple velocities, particularly when multiple targets lie at the same range, a Doppler FFT is performed across multiple chirps (forming a "chirp frame") to extract consistent inter-chirp phase changes. This results in a velocity spectrum where peaks correspond to distinct Doppler velocities.

Limitation of FFT in Vibrational Motion. While FFT is effective for estimating constant or slowly varying velocities, it fails in the presence of high-frequency vibrational motion. In such cases, the radial velocity of the object is a time-varying signal, often oscillatory in nature. For instance, consider an object vibrating harmonically:

$$v(t) = Acos(2\pi f_v t) \tag{4}$$

This velocity profile leads to a time-varying phase in the received signal:

$$\phi(t) = \int_0^t v(\tau)\, d\tau = \frac{A}{2\pi f_v} \sin(2\pi f_v t) \tag{5}$$

The resulting IF signal is no longer a pure sinusoid or even a sum of discrete sinusoids. Instead, the radar output contains a cosine of a cosine, which is a nonlinear and non-stationary signal. The Fourier Transform of such a function yields a spread of energy across many frequency bins, often with aliasing and distortion, making FFT-based methods unsuitable for precise frequency recovery in this context.

This motivates the need for a new methodology capable of resolving instantaneous frequency variations introduced by micro-vibrations, which cannot be captured by standard Doppler FFT pipelines.

3.2. IQ Data and Time-Domain Vibration Recovery

Given the limitations of Fourier-based methods in capturing non-linear or high-frequency motion, we instead analyze the raw radar data: the in-phase and quadrature (IQ) signals. These are the complex-valued outputs from the mixer after analog-to-digital conversion, recorded prior to Doppler FFT processing.

mmWave radar typically employs frequency-modulated continuous wave (FMCW) chirp signals for distance measurement, as illustrated in Fig. 3(a). The frequency difference between the transmitted signal (Tx) and the received signal (Rx) reflects the signal propagation time, which can be used to estimate the object distance. Letting $R(t)$ denote the time-varying distance between the antenna and the vibrating object, the transmitted and received signals can be expressed as:

$$S_{T_x}(t) = \exp\left[j\left(2\pi f_c t + \pi K t^2\right)\right], \tag{6}$$

$$S_{R_x}(t) = \alpha S_{T_x}\left(t - \frac{2R(t)}{c}\right), \tag{7}$$

where α is the path loss, f_c is the starting frequency, and K is the chirp slope of the FMCW signal.

After mixing the transmitted and received signals, we obtain the so-called beat signal $s(t)$:

$$s(t) = S_{T_x}(t) S^*_{R_x}(t) \approx \alpha \exp\left[j4\pi \frac{(f_c + Kt)R(t)}{c}\right], \tag{8}$$

where the phase encodes the distance information $R(t)$. We focus on the real part of this signal:

$$s_{\text{real}}(t) = \alpha \cos\left(4\pi \frac{(f_c + Kt)R(t)}{c}\right). \tag{9}$$

We consider three scenarios:

1. Static Object
   If the object is static, $R(t)$ is a constant R_0. Then the frequency of the signal is $\frac{4\pi K R_0}{c}$ and phase offset of it is $\frac{4\pi f_c R_0}{c}$, both of them are constant. Thus, the radar raw signal exhibits horizontal lines, as shown in Fig.1.
2. Constant-Speed Motion.
   If the object moves at a constant velocity v, then:

$$R(t) = R_0 + vt. \tag{10}$$

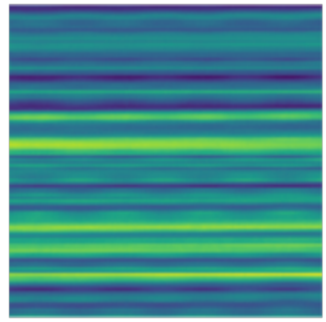

Figure 1

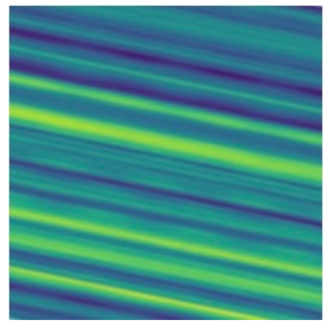

Figure 2

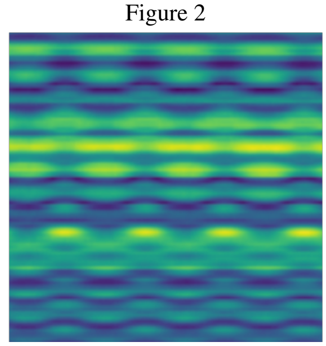

Figure 3

Substituting into the signal:

$$s(t)_{real} = \alpha \cos(4\pi \frac{(f_c + Kt)R(t)}{c}) \tag{11}$$

$$= \alpha \cos(\frac{4\pi}{c}(f_c + Kt)(R_0 + vt)) \tag{12}$$

$$= \alpha \cos(\frac{4\pi}{c}(f_c + Kt_f)(R_0 + v(t_f + t_s))) \tag{13}$$

$$= \alpha \cos(\frac{4\pi}{c}(f_c R_0 + f_c v t_f + f_c v t_s + \tag{14}$$

$$K t_f R_0 + K t_f v t_f + K t_f v t_s) \tag{15}$$

Assuming the chirp duration is short (i.e., Kt^2 is negligible compared to other terms), we approximate:

$$s(t)_{real} \approx \alpha \cos(\frac{4\pi}{c}(f_c R_0 + f_c v t_f + f_c v t_s + K t_f R_0) \tag{16}$$

So the frequency and the phase of the signal are:

$$\text{Frequency} = \frac{4\pi}{c}(f_c v + KR_0) \tag{17}$$

$$\text{Phase} = \frac{4\pi}{c}(f_c R_0 + f_c v t_s) \tag{18}$$

Therefore, the radar raw signal appears as diagonal lines, which is shown in Fig.2.

3. Vibrating Object.
When the object vibrates, we model its displacement as a sinusoidal function $x(t)$. The distance becomes:

$$R(t) = R_0 + x(t), \tag{19}$$

and the phase evolves as:

$$\text{Phase} = \frac{4\pi f_c}{c}(R_0 + x(t)). \tag{20}$$

Substituting back into the signal, we find that the observed waveform becomes a cosine of a cosine, a highly non-linear signal. Consequently, traditional Fourier analysis becomes invalid. Instead, the raw signal itself exhibits a clear sinusoidal pattern, directly revealing the object's vibration frequency, as shown in Fig.3. In particular, the number of visible cycles within a fixed observation window reveals the vibration frequency. For instance, if three full oscillations are observed within one radar frame (frame period $T_f = 0.1$ s), the vibration frequency is:

$$f_v = \frac{3}{T_f} = 30 \text{ Hz}. \tag{21}$$

4. Experiments

4.1. Settings

The Chladni Plate. To systematically explore vibration frequency recovery using mmWave radar, we first construct a controlled experimental setup centered around a Chladni plate (illustrated in Fig.4). A Chladni plate is a thin, flat metal plate commonly used in physics and acoustics to visualize the vibration modes of a surface. When driven at specific frequencies, the plate resonates and forms distinctive nodal patterns where the surface remains stationary, while other regions vibrate.

In our setup, the Chladni plate is connected to a motorized actuator that allows precise control over both the vibration frequency and amplitude. This enables us to conduct repeatable experiments under various motion conditions, ensuring a controlled environment to test and validate our radar-based vibration sensing method.

Sensor Rig. For sensing, we employ a pre-calibrated multi-sensor rig composed of a mmWave radar, a camera, and a LiDAR sensor (shown in Fig. 5). All three sensors are

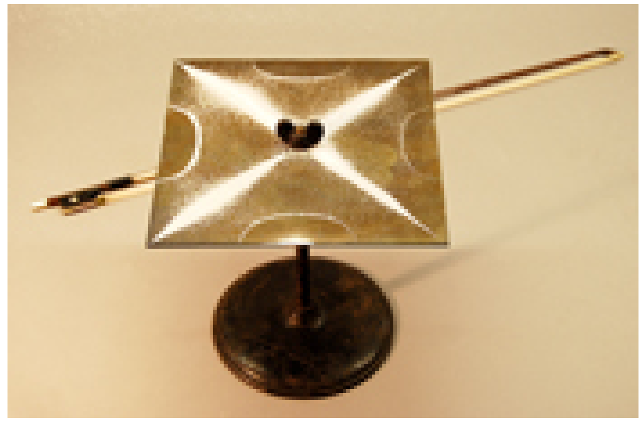

Figure 4. The Chladni Plate.

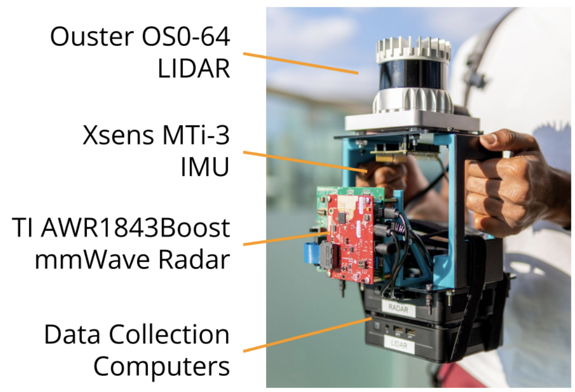

Figure 5. Handheld data collection system.

spatially aligned and synchronized to capture multi-modal data from the same viewpoint. While our main focus is on radar-based vibration analysis, the additional camera and LiDAR data provide supplementary validation and environmental context during experiments.

4.2. Experimental Results

Can Radar Detect the Presence of Vibration? To investigate whether mmWave radar can detect vibration, we operate the radar in FMCW mode and extract Range-Doppler representations from the raw in-phase and quadrature (I/Q) data. A Range-Doppler map is a two-dimensional matrix that shows the strength of reflected signals as a function of both distance (Range) and radial velocity (Doppler). Each pixel in the map represents the intensity of the returned signal at a specific combination of range and velocity. Range-Doppler processing is a standard tool in radar systems for separating stationary and moving objects and is particularly useful for observing periodic motion such as vibration.

We design a series of step-by-step experiments to understand how vibration appears in Range-Doppler space:

1. Static Plate.
We keep the Chladni plate completely stationary. In this

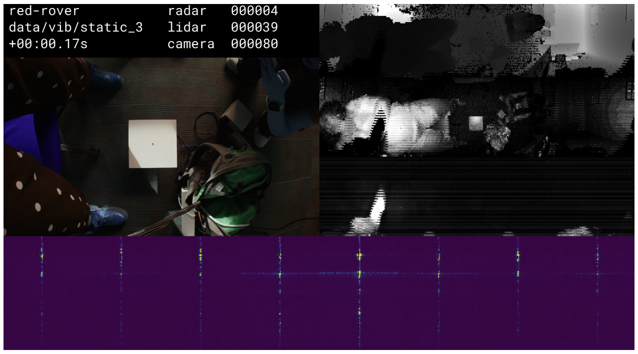

Figure 6. Range-Doppler map with the Chladni plate held completely stationary. Top-left: visualization from the camera, capturing the scene in the RGB domain. Top-right: visualization from the LiDAR sensor, providing dense 3D point cloud information. Bottom: raw radar signal captured using an 8-antenna mmWave radar, illustrating radar reflections across spatial channels. A single strong vertical line centered at zero Doppler is observed, corresponding to the static reflection from the plate.

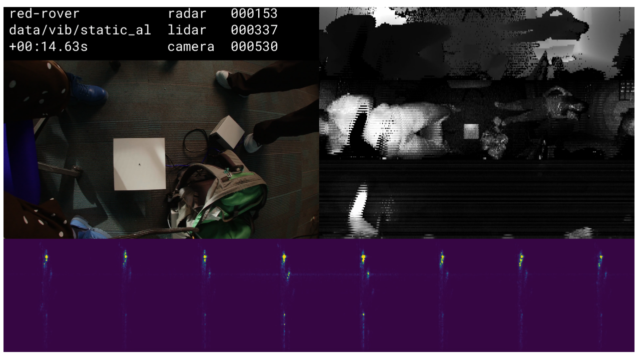

Figure 7. Range-Doppler map when the radar sensor is manually moved forward and backward while the Chladni plate remains stationary. The observed horizontal displacement reflects the Doppler shift introduced by the relative motion between the radar and the target.

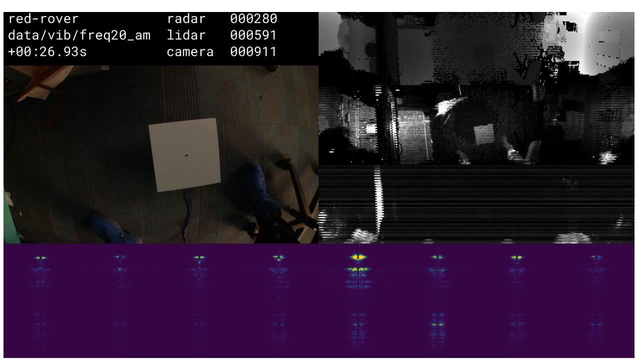

Figure 8. Range-Doppler map of the Chladni plate vibrating at a fixed amplitude with varying vibration frequencies. Periodic sidebands appear around the zero-Doppler line, reflecting the oscillatory motion of the plate.

case, we expect to observe a single strong response at zero Doppler shift, corresponding to the static reflection from the plate. As shown in Fig.6, we indeed see a vertical line centered at zero Doppler, confirming the static nature of the target.

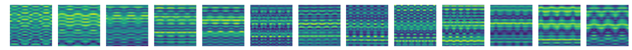

Figure 9. Raw radar signal captured as the Chladni plate vibrates with varying frequencies. The vibration frequency is swept from 20 Hz to 60 Hz and then back to 20 Hz, while maintaining a constant vibration amplitude.

2. Moving Radar.
   Next, we hold the plate stationary but manually move the radar sensor forward and backward. This movement introduces a Doppler shift due to the relative velocity between the radar and the target. As expected, Fig.7 shows a horizontal displacement in the Range-Doppler map, corresponding to the introduced velocity.
3. Vibrating Plate.
   Finally, we vibrate the Chladni plate at a fixed amplitude while varying the vibration frequency. In this case, we expect that the periodic motion will induce oscillatory Doppler signatures. Fig.8 illustrates the resulting Range-Doppler image, where periodic sidebands appear around the zero-velocity line, indicating the presence of vibration. These oscillations become more pronounced as the vibration frequency increases.

Through these controlled tests, we confirm that mmWave radar is capable of detecting the presence of vibration, even without relying on additional sensors.

Recovering Vibration Frequency. Beyond merely detecting vibration, we also aim to recover the vibration frequency directly from the radar's raw I/Q data. As previously discussed, the vibration frequency is encoded in the phase variations of the radar return signal.

To demonstrate this, we conduct an experiment where the Chladni plate vibrates with varying frequencies, while maintaining a constant vibration amplitude. Specifically, we sweep the frequency from 20 Hz up to 60 Hz and then back down to 20 Hz. The resulting raw radar signal is shown in Fig.9.

In the figure, the number of oscillations (peaks) observed within a fixed time window directly reflects the vibration frequency. At the beginning (20 Hz), we observe approximately two cycles. As the frequency increases to 60 Hz, the number of cycles increases correspondingly to about six, before decreasing back to two cycles when the frequency returns to 20 Hz.

This experiment clearly demonstrates that by counting the number of peaks or analyzing the periodicity in the raw radar signal, we can accurately recover the vibration frequency of the object.

5. Conclusion

In this project, we investigate the use of mmWave FMCW radar for recovering vibration frequency without relying on traditional Fourier-based methods. By directly analyzing raw in-phase and quadrature (IQ) signals, we are able to capture subtle, non-linear, and high-frequency vibrational motion that would otherwise be distorted or lost in Doppler FFT processing. Through a series of controlled experiments using a Chladni plate, we demonstrate that vibration signatures are clearly observable in the time-domain radar signals, and that the vibration frequency can be accurately recovered by examining the number of oscillatory cycles. Our approach reveals the potential of mmWave radar as a low-cost sensing modality for high-precision vibration analysis, opening up new possibilities for applications in structural monitoring, robotics, and industrial inspection.

References

[1] Heba Abdelnasser and Moustafa Youssef. Wi-vib: Estimating vibration using wifi. In *IEEE INFOCOM 2020 - IEEE Conference on Computer Communications*, pages 1604–1613, 2020. 1

[2] Huijie Chen, Fan Li, and Yu Wang. Echotrack: Acoustic device-free hand tracking on smart phones. In *IEEE INFOCOM 2017-IEEE Conference on Computer Communications*, pages 1–9. IEEE, 2017. 1

[3] Tianbo Gu, Zheng Fang, Zhicheng Yang, Pengfei Hu, and Prasant Mohapatra. Mmsense: Multi-person detection and identification via mmwave sensing. In *Proceedings of the 3rd ACM Workshop on Millimeter-wave Networks and Sensing Systems*, pages 45–50, 2019. 2

[4] Chengkun Jiang, Junchen Guo, Yuan He, Meng Jin, Shuai Li, and Yunhao Liu. mmvib: micrometer-level vibration measurement with mmwave radar. In *Proceedings of the 26th Annual International Conference on Mobile Computing and Networking*, pages 1–13, 2020. 1, 2

[5] Ping Li, Zhenlin An, Lei Yang, and Panlong Yang. Towards physical-layer vibration sensing with rfids. In *IEEE INFOCOM 2019-IEEE Conference on Computer Communications*, pages 892–900. IEEE, 2019. 1

[6] Jian Liu, Yan Wang, Gorkem Kar, Yingying Chen, Jie Yang, and Marco Gruteser. Snooping keystrokes with mm-level audio ranging on a single phone. In *Proceedings of the 21st Annual International Conference on Mobile Computing and Networking*, pages 142–154, 2015. 1

[7] Jian Liu, Yingying Chen, Marco Gruteser, and Yan Wang. Vibsense: Sensing touches on ubiquitous surfaces through vibration. In *2017 14th Annual IEEE International Conference on Sensing, Communication, and Networking (SECON)*, pages 1–9. IEEE, 2017. 1

[8] Qifan Pu, Sidhant Gupta, Shyamnath Gollakota, and Shwetak Patel. Whole-home gesture recognition using wireless signals. In *Proceedings of the 19th annual international conference on Mobile computing & networking*, pages 27–38, 2013. 1

[9] Lorenzo Scalise, Yanguang Yu, Guido Giuliani, Guy Plantier, and Thierry Bosch. Self-mixing laser diode velocimetry: application to vibration and velocity measurement. *IEEE Transactions on instrumentation and measurement*, 53(1):223–232, 2004. 1

[10] Anran Wang and Shyamnath Gollakota. Millisonic: Pushing the limits of acoustic motion tracking. In *Proceedings of the 2019 CHI conference on human factors in computing systems*, pages 1–11, 2019. 2

[11] Feng Zhang, Chenshu Wu, Beibei Wang, and KJ Ray Liu. mmeye: Super-resolution millimeter wave imaging. *IEEE Internet of Things Journal*, 8(8):6995–7008, 2020. 2